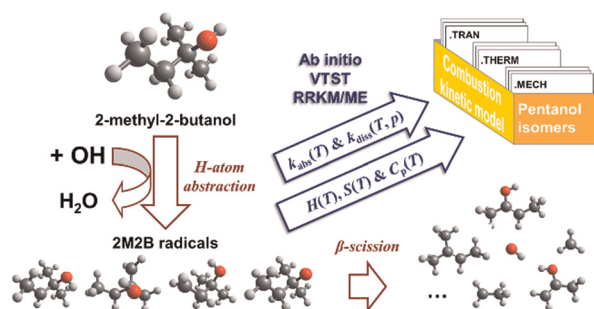


Please use this PDF proof to check the layout of your article. If you would like any changes to be made to the layout, you can leave instructions in the online proofing interface. First, return to the online proofing interface by clicking "Edit" at the top page, then insert a Comment in the relevant location. Making your changes directly in the online proofing interface is the quickest, easiest way to correct and submit your proof.

Please note that changes made to the article in the online proofing interface will be added to the article before publication, but are not reflected in this PDF proof.

We have presented the graphical abstract image and text for your article below. This briefly summarises your work, and will be presented with your article online.



An *ab initio* kinetics study on 2-methyl-2-butanol oxidation induced by •OH radicals

Shuyan Guo, Yuxiang Zhu, Hao Zhao* and Chong-Wen Zhou*

Rate constants and thermochemical data for H-atom abstraction reactions from 2-methyl-2-butanol by hydroxyl radicals and the subsequent β -scission reactions of the product radicals were calculated.

Q3

Please check this proof carefully. Our staff will not read it in detail after you have returned it.

Please send your corrections either as a copy of the proof PDF with electronic notes attached or as a list of corrections. **Do not edit the text within the PDF or send a revised manuscript** as we will not be able to apply your corrections. Corrections at this stage should be minor and not involve extensive changes.

Proof corrections must be returned as a single set of corrections, approved by all co-authors. No further corrections can be made after you have submitted your proof corrections as we will publish your article online as soon as possible after they are received.

Please ensure that:

- The spelling and format of all author names and affiliations are checked carefully. You can check how we have identified the authors' first and last names in the researcher information table on the next page. **Names will be indexed and cited as shown on the proof, so these must be correct.**
- Any funding bodies have been acknowledged appropriately and included both in the paper and in the funder information table on the next page.
- All of the editor's queries are answered.
- Any necessary attachments, such as updated images or ESI files, are provided.

Translation errors can occur during conversion to typesetting systems so you need to read the whole proof. In particular please check tables, equations, numerical data, figures and graphics, and references carefully.

Please return your **final** corrections, where possible within **48 hours** of receipt following the instructions in the proof notification email. If you require more time, please notify us by email to pccp@rsc.org.

Funding information

Providing accurate funding information will enable us to help you comply with your funders' reporting mandates. Clear acknowledgement of funder support is an important consideration in funding evaluation and can increase your chances of securing funding in the future.

We work closely with Crossref to make your research discoverable through the Funding Data search tool (<http://search.crossref.org/funding>). Funding Data provides a reliable way to track the impact of the work that funders support. Accurate funder information will also help us (i) identify articles that are mandated to be deposited in **PubMed Central (PMC)** and deposit these on your behalf, and (ii) identify articles funded as part of the **CHORUS** initiative and display the Accepted Manuscript on our web site after an embargo period of 12 months.

Further information can be found on our webpage (<http://rsc.li/funding-info>).

What we do with funding information

We have combined the information you gave us on submission with the information in your acknowledgements. This will help ensure the funding information is as complete as possible and matches funders listed in the Crossref Funder Registry.

If a funding organisation you included in your acknowledgements or on submission of your article is not currently listed in the registry it will not appear in the table on this page. We can only deposit data if funders are already listed in the Crossref Funder Registry, but we will pass all funding information on to Crossref so that additional funders can be included in future.

Please check your funding information

The table below contains the information we will share with Crossref so that your article can be found *via* the Funding Data search tool. **Please check that the funder names and grant numbers in the table are correct and indicate if any changes are necessary to the Acknowledgements text.**

Funder name	Funder's main country of origin	Funder ID (for RSC use only)	Award/grant number
National Science and Technology Major Project	China	501100018537	2017-III-0004-0028
Sinopec Ministry of Science and Technology Basic Prospective Research Project	China	501100013154	Unassigned
Beihang University	China	501100002358	Unassigned

Q1

Researcher information

Please check that the researcher information in the table below is correct, including the spelling and formatting of all author names, and that the authors' first, middle and last names have been correctly identified. **Names will be indexed and cited as shown on the proof, so these must be correct.**

If any authors have ORCID or ResearcherID details that are not listed below, please provide these with your proof corrections. Please ensure that the ORCID and ResearcherID details listed below have been assigned to the correct author. Authors should have their own unique ORCID iD and should not use another researcher's, as errors will delay publication.

Please also update your account on our online [manuscript submission system](#) to add your ORCID details, which will then be automatically included in all future submissions. See [here](#) for step-by-step instructions and more information on author identifiers.

First (given) and middle name(s)	Last (family) name(s)	ResearcherID	ORCID iD
Shuyan	Guo		
Yuxiang	Zhu		
Hao	Zhao		
Chong-Wen	Zhou		0000-0003-0845-988X

Queries for the attention of the authors

Journal: PCCP

Paper: d2cp02164a

Title: **An *ab initio* kinetics study on 2-methyl-2-butanol oxidation induced by •OH radicals**

For your information: You can cite this article before you receive notification of the page numbers by using the following format: (authors), Phys. Chem. Chem. Phys., (year), DOI: 10.1039/d2cp02164a.

Editor's queries are marked on your proof like this **Q1**, **Q2**, etc. and for your convenience line numbers are indicated like this 5, 10, 15, ...

Please ensure that all queries are answered when returning your proof corrections so that publication of your article is not delayed.

Query reference	Query	Remarks
Q1	Funder details have been incorporated in the funder table using information provided in the article text. Please check that the funder information in the table is correct and indicate any changes, if required. If changes are required, please ensure that you also amend the Acknowledgements text as appropriate.	
Q2	Have all of the author names been spelled and formatted correctly? Names will be indexed and cited as shown on the proof, so these must be correct. No late corrections can be made.	
Q3	The article title has been altered for clarity. Please check that the meaning is correct.	
Q4	Please note that a conflict of interest statement is required for all manuscripts. Please read our policy on Conflicts of interest (http://rsc.li/conflicts) and provide a statement with your proof corrections. If no conflicts exist, please state that "There are no conflicts to declare".	
Q5	Have all of the funders of your work been fully and accurately acknowledged? If not, please ensure you make appropriate changes to the Acknowledgements text	

An *ab initio* kinetics study on 2-methyl-2-butanol oxidation induced by $\cdot\text{OH}$ radicals†

Shuyan Guo,^{‡a} Yuxiang Zhu,^{‡b} Hao Zhao^{*a} and Chong-Wen Zhou^{id} ^{*bc}

High-level *ab initio* calculations were performed to investigate the kinetics of the important initial steps of 2-methyl-2-butanol (2M2B) oxidation. Hydrogen-atom abstraction reactions by hydroxyl ($\cdot\text{OH}$) radicals, dehydration reactions of 2M2B molecules, and unimolecular isomerization and decomposition reactions of 2M2B radicals produced by H-atom abstraction were all included in this work. The potential energy surfaces were characterized at the QCISD(T)/CBS//M06-2X/6-311++G(d,p) level of theory. Variational transition state theory (VTST) was employed to calculate the rate coefficients for the H-atom abstraction reactions. It is interesting to note that the hydrogen bond formed in the transition state (TS) in H-atom abstraction reactions, leading to a ring-shaped structure, has a large influence on the electronic energy barriers and rotational–vibrational properties of the TS and thus the rate coefficients. For comparison, rate coefficient calculations were carried out for the same reaction channel by employing different types of TS structures separately, with or without hydrogen bonds. For all the unimolecular reactions studied here, pressure-dependent rate coefficients were obtained through Rice–Ramsperger–Kassel–Marcus/master equation (RRKM/ME) calculations at pressures of 0.01–100 atm. In addition, thermochemical properties at temperatures from 300 to 3000 K for all the species in the title reactions were calculated, which were found to be in good agreement with literature data. The kinetics and thermochemical data calculated in this study are important in predicting the combustion properties of 2M2B, which can be used in the combustion kinetic model development of 2M2B oxidation.

Received 13th May 2022,
Accepted 19th September 2022

DOI: 10.1039/d2cp02164a

rsc.li/pccp

1. Introduction

Combustion has long served as an important source of energy for human society. However, fossil fuels which are predominantly used are not sustainable due to their limited reserves and are also not eco-friendly. There is increasing focus on using alcohol fuels, which can be sustainably produced from biomass and are demonstrated to have favourable combustion properties as potential alternative fuels or as additives to conventional fuels.¹ Experimental and modeling studies have been performed extensively to explore the combustion chemistry of alcohols. Sarathy *et al.*² provided a comprehensive review of alcohol combustion chemistry and it can be seen that the published studies on the oxidation of alcoholic species in the

past decade mainly focused on alcohols from C_1 to C_4 . However, the superiority of pentanol molecules as alternative fuels for internal combustion engines over smaller alcohol molecules was demonstrated.² For example, pentanols have higher carbon and hydrogen contents and thus higher LHVs similar to gasoline. They also have higher boiling points and thus have less impact on the fuel distillation curve as additives; they have a lower specific latent heat of vaporization and are therefore easier to ignite under cold-start operating conditions, *etc.* The feasibility of pentanol isomers as alternative fuels has been demonstrated by motor-scale experiments, *e.g.*, an HCCI engine test conducted by Yang *et al.*³ In addition, Lapuerta *et al.*⁴ found that short-chain alcohols exhibit poor blending stability and low viscosity. Compared to alcohols from C_1 to C_4 , pentanol is more suitable to be blended with diesel fuel. Some other studies found that a higher *n*-pentanol ratio can reduce the natural luminosity of spray combustion and lead to simultaneous reduction of NO_x ⁵ and soot emissions,⁶ and improved thermal efficiency. Efficient production routes for pentanol isomers, for example, through engineered microorganisms,⁷ have been explored.

To understand the combustion reaction mechanism of pentanol isomers, a number of experimental and modeling studies have been carried out. A recent review by Cai *et al.*⁸

^a College of Engineering, Peking University, Beijing 100871, P. R. China.
E-mail: h.zhao@pku.edu.cn

^b School of Energy and Power Engineering, Beihang University, Beijing 100191, P. R. China. E-mail: cwzhou@buaa.edu.cn

^c Combustion Chemistry Centre, School of Biological and Chemical Science, Ryan Institute, University of Galway, Galway H91TK33, Ireland

† Electronic supplementary information (ESI) available: The calculated rate coefficients and thermochemical data. See DOI: <https://doi.org/10.1039/d2cp02164a>

‡ These authors contributed equally to this work.

focused on the combustion kinetics of higher linear alcohols where the experimental studies, for mainly *n*-pentanol, were summarized, and connections between the combustion behaviours observed from combustion experiments with the combustion kinetics governed by the chain length and functional groups of higher alcohols were discussed in detail. Earlier in the last decade, Heufer *et al.*⁹ developed a kinetic model for 1-pentanol based on the previously proposed rate rules for *n*-butanol and used the measured auto-ignition and speciation data to validate their model. Dagaut and co-workers employed jet-stirred reactors (JSR) to study the oxidation mechanisms of a series of pentanol isomers, including 1-pentanol,¹⁰ 2-methyl-1-butanol¹¹ and 3-methyl-1-butanol.¹² More recently, Köhler *et al.*¹³ systematically investigated the oxidation pathways of *n*-pentanol in laminar, flat, low-pressure H₂/O₂/Ar based flames doped with equal amounts of pre-vaporized alcohols. Cao *et al.*¹⁴ studied the pyrolysis of *n*-pentanol and 2-methyl-1-butanol in a flow reactor and developed a kinetic model to validate against their measurements. Experimental and modeling efforts have been devoted comprehensively to understanding the oxidation mechanisms of *n*-pentanol and 2-methyl-1-butanol in recent years, whereas investigations on 2-methyl-2-butanol combustion are quite limited in the literature.^{15,16} 2-Methyl-2-butanol is the only tertiary pentanol isomer, and studies on the kinetics of 2-methyl-2-butanol oxidation will be helpful to understanding the combustion chemistry of higher *tert*-amyl alcohols and eventually beneficial for choosing the pentanol isomer with correct isomeric properties.

H-atom abstraction, dehydration reactions of alcohol molecules, and subsequent isomerization and decomposition reactions of alcohol radicals are important initial steps among the ~30 reaction classes of alcohol oxidation.² Zhao *et al.*¹⁷ carried out *ab initio* calculations for the thermal decomposition of 1-pentanol, 2-methyl-1-butanol and 3-methyl-1-butanol at the CBS-QB3 level and obtained the pressure-dependent rate coefficients from the solutions of the master equation. Aazaad *et al.*¹⁸ calculated the rate coefficients at temperatures from 270 to 350 K for the α H-atom abstraction reactions of *n*-pentanol isomers by \bullet OH radicals using VTST. Van de Vijver *et al.*¹⁹ studied the potential energy surfaces for the decomposition and isomerization reactions of 1-pentanol radicals at the UCCSD(T)-F12a/cc-pVTZ-F12//M06-2X/6-311++G(d,p) level of theory, and calculated the rate coefficients by solving the master equation. Xing *et al.*²⁰ implemented multi-path variational transition state theory (MP-VTST) to calculate the rate coefficients of H-atom abstraction of 3-methyl-1-butanol by \bullet OH radicals. Bai *et al.*²¹ investigated the kinetics of the decomposition and isomerization reactions of 2-pentanol-2-yl radicals at the ROCCSD(T)/CBS//B2PLYPD3/6-311++G(d,p) level of theory, and calculated the thermochemical properties of the important species involved in the reaction process. Bai *et al.*²² studied the energetics of the H-atom abstraction reactions of 1-pentanol, 2-pentanol, and 3-pentanol by hydroxyl radicals at the CCSD(T)/CBS//M06-2X/6-311+G(d,p) level and calculated the rate coefficients by using the multi-structural variational transition state theory (MS-VTST) together with small curvature

tunnelling (SCT) correction. To date, the kinetics of the initial oxidation steps of 2-methyl-2-butanol have not been investigated either experimentally or theoretically.

In this study, the kinetics of the important primary oxidation steps of 2-methyl-2-butanol (2M2B), including hydrogen-atom abstraction reactions by hydroxyl (\bullet OH) radicals, dehydration reactions of 2M2B, and the isomerization and β -scission reactions of 2M2B radicals, were investigated theoretically. In addition, the thermochemical properties of all the species involved were also calculated. This study aims to provide accurate kinetics and thermochemical data for the important reaction classes of 2M2B oxidation which can be used in the model development for 2M2B oxidation.

2. Computational method

2.1. Potential energy surfaces

The molecular structures of all the species and transition states (TS) involved in the title reactions were optimized using the M06-2X²³ method with the 6-311++G(d,p)²⁴ basis set. The frequencies of all normal vibrational modes and the zero-point energy (ZPE) corrections were obtained at the same level of theory. Intrinsic reaction coordinate (IRC) calculations were also carried out at the M06-2X/6-311++G(d,p) level, in order to confirm that each TS connects the desired reactants and products, and to obtain the molecular properties of a number of transition structures along the reaction coordinate for the reactions with a loose TS. One-dimensional hindered rotor approximation was applied for the low-frequency torsional modes of all species and TSs, with their hindrance potentials scanned at the M06-2X/6-31G level of theory. Single-point energies for all stationary points on the potential energy surfaces (PES) were calculated by using the quadratic configuration interaction method with singles, doubles and perturbative inclusion of triples, QCISD(T),²⁵ with Dunning's cc-pVDZ²⁶ and cc-pVTZ²⁷ basis sets, and the MP2²⁸ method with the cc-pVDZ,²⁶ cc-pVTZ²⁷ and cc-pVQZ²⁹ basis sets. Then the QCISD(T) and MP2 energies were extrapolated to the complete basis set (CBS) limit *via* the expressions:³⁰

$$E_{\text{QCISD(T)/CBS, DZ} \rightarrow \text{TZ}} = E_{\text{QCISD(T)/TZ}} + (E_{\text{QCISD(T)/TZ}} - E_{\text{QCISD(T)/DZ}}) \times 0.4629 \quad (1)$$

$$E_{\text{MP2/CBS, TZ} \rightarrow \text{QZ}} = E_{\text{MP2/QZ}} + (E_{\text{MP2/QZ}} - E_{\text{MP2/TZ}}) \times 0.6938 \quad (2)$$

$$E_{\text{MP2/CBS, DZ} \rightarrow \text{TZ}} = E_{\text{MP2/TZ}} + (E_{\text{MP2/TZ}} - E_{\text{MP2/DZ}}) \times 0.4629 \quad (3)$$

$$E_{\text{QCISD(T)/CBS}} = E_{\text{QCISD(T)/CBS, DZ} \rightarrow \text{TZ}} + E_{\text{MP2/CBS, TZ} \rightarrow \text{QZ}} - E_{\text{MP2/CBS, DZ} \rightarrow \text{TZ}} \quad (4)$$

The electronic structure and single point energy calculations in this study were performed by using the Molpro 2015³¹ program.

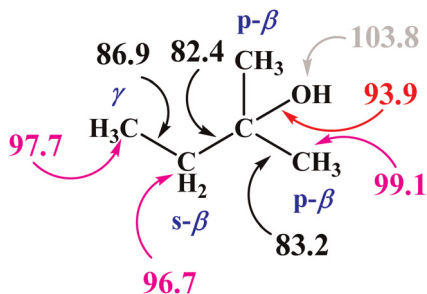


Fig. 1 Definitions of different carbon sites on 2-methyl-2-butanol (2M2B) with "p-β" denoting the primary beta site and "s-β" denoting the secondary beta site, and bond dissociation energies at 0 K (kcal mol^{-1}) calculated at the G4⁴¹ level of theory.

2.2. Rate coefficient calculations

In this study, variational transition state theory (VTST) was employed to calculate the rate coefficients for the H-atom abstraction reactions by $\bullet\text{OH}$ radicals because of their relatively small energy barriers of $\sim 1.5 \text{ kcal mol}^{-1}$ or submerged TSs below the reactants in energy. The Hessians of the transition structures along the minimum energy path obtained from IRC calculations were employed to calculate the normal mode vibrational frequencies and the ZPEs using the ProjRot code from the Auto-Mech program suite.³² On the other hand, the reaction kinetics of the dehydration reactions of 2M2B, and the isomerization and decomposition reactions of 2M2B radicals were explored by performing the Rice–Ramsperger–Kassel–Marcus/master equation (RRKM/ME) calculations, in order to obtain pressure-dependent rate coefficients in the pressure range of 0.01–100 atm with N_2 as the bath gas. For all the reactions investigated in this study, the Master Equation System Solver (MESS)³³ program was used to calculate the rate coefficients, with the rigid-rotor-harmonic-oscillator (RRHO) model employed to characterize the rotational-vibrational degrees of freedom, while 1-D hindered rotor approximation was applied for the torsional modes. The asymmetric Eckart model³⁴ was applied to quantify the tunnelling effects. In the master equation modeling, the collisional frequency was modeled by using the Lennard–Jones (L-J) potential,³⁵ with the parameters $\sigma = 3.6 \text{ \AA}$, $\varepsilon = 68 \text{ cm}^{-1}$ for N_2 and $\sigma = 6.27 \text{ \AA}$, $\varepsilon = 341.3 \text{ cm}^{-1}$ employed for another $\text{C}_5\text{H}_{11}\text{O}$ system²¹ adopted here for the 2M2B and 2M2B radicals by analogy. The exponential-down model³⁶ was employed to describe collisional energy relaxation, with the average downward energy transferred per collision estimated as $\langle \Delta E_{\text{down}} \rangle = 200 \times (T/300)^{0.75} \text{ cm}^{-1}$.²¹ The calculated phenomenological rate coefficients for title reactions were fitted by modified Arrhenius expression and are provided in the ESI.†

2.3. Thermochemical calculations

The molecular partition functions calculated by using the MESS³³ code were employed to compute the temperature-dependent enthalpies (H), entropies (S) and heat capacities (C_p) for all the species involved in the title reactions *via* calls to the ThermP³⁷ code. The enthalpies of formation at 0 K for all

Table 1 Saddle point geometries employed for H-atom abstraction reactions from the carbon sites obtained at the M06-2X/6-311++G(d,p) level of theory (with atomic distances in units of \AA)

With hydrogen bond	Without hydrogen bond
<p>"p-β"</p>	<p>"p-β"</p>
<p>"s-β"</p>	<p>"s-β"</p>
<p>"γ"</p>	<p>"γ"</p>

species were calculated based on the atomization approach by using CBS-APNO,³⁸ CBS-QB3,³⁹ G3,⁴⁰ and G4⁴¹ composite methods and taking the average, which showed good agreement (rivalling "chemical accuracy", 1 kcal mol^{-1}) with the ATcT benchmarked formation enthalpies for some 50 $\text{C}_x\text{H}_y\text{O}_z$ molecules.⁴² The calculated thermochemical properties at temperatures from 300 to 3000 K were finally fitted by NASA polynomials through the PAC99⁴³ program and are provided in the ESI.†

3. Results and discussion

3.1. H-atom abstraction reactions by $\bullet\text{OH}$ radicals

As illustrated in Fig. 1, relative to the hydroxyl group, the 2M2B molecule has two primary β sites (p-β), one secondary β (s-β) site and one γ site, from which a hydrogen atom can be abstracted and four different radicals, namely, 2-methyl-2-butoxy, 2M2B-1-yl, 2M2B-3-yl and 2M2B-4-yl, can be produced. The bond dissociation energy (BDE) for the C–H bond at the s-β site is the lowest, while the BDE for the O–H bond is $\sim 5 \text{ kcal mol}^{-1}$ higher than those for the C–H bonds. It is important to note that, except for the TS of the H-atom abstraction reaction from the hydroxyl group, a hydrogen bond could be formed between the hydroxyl group and $\bullet\text{OH}$ radical in the TSs of the other three H-atom abstraction reaction pathways by the $\bullet\text{OH}$

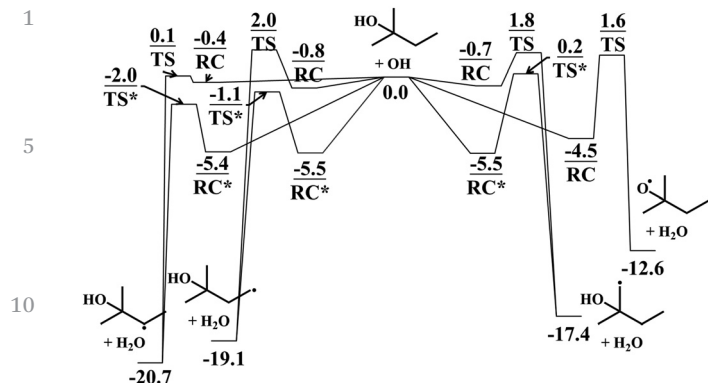


Fig. 2 ZPE corrected PESs (in units of kcal mol^{-1}) for the H-atom abstraction reactions from 2M2B by $\bullet\text{OH}$ at the QCISD(T)/CBS//M06-2X/6-311++G(d,p) level. "TS" denotes the transition state, "RC" denotes the van der Waals pre-reaction complex and asterisks mark the TSs with hydrogen bonds.

radical, leading to a ring-shaped structure. As discussed by Rotavera and Taatjes,⁴⁴ the effects of hydrogen bonding in TSs lead to differences in the rate coefficients and branching fractions of the initial oxidation steps, which could have a pronounced influence on the combustion kinetics of oxygenated species at lower temperatures. Transition state geometries with and without hydrogen bonds for the same position are shown in Table 1 and the hydrogen bonds are typically ~ 2.0 Å which will lower the electronic energy barrier. With different geometries, partition functions for the TSs with or without hydrogen bonds, calculated with the RRHO treatment for the rotational and vibrational degrees of freedom and 1-D hindered rotor descriptions for the internal torsional modes, are also quite different. Moreover, since the formation of a ring converts the internal rotational degrees of freedom to ring vibrations and eventually leads to lower entropy,⁴⁵ it is considered less favorable under combustion temperature regimes. In order to investigate the effect of hydrogen bond formation in the TS on reaction kinetics, rate coefficients for the H-atom abstraction reactions from the p- β , s- β and γ sites were calculated by using the TS structures with and without hydrogen bonds and are shown in Table 1 separately. Different electronic energy barriers and rotational-vibrational properties corresponding to the different TS geometries were used in the rate constant calculations for comparison.

The relative electronic energies to the reactants, 2M2B + $\bullet\text{OH}$, for all stationary points on the PESs of the H-atom abstraction reactions are shown in Fig. 2. A pre-reaction van der Waals complex was located for each reaction channel. The reactants will undergo a barrier-less reaction channel to form the van der Waals complex, and then surmount the inner TS barrier to finally become the bimolecular products. Since the bottleneck of reactive fluxes is at the inner TS and the kinetic effect of the barrier-less entrance reaction channel is negligible at temperatures above 300 K,^{46,47} a one-TS model including only the inner TS is expected to be sufficient for the rate coefficient calculations here. The energy differences between

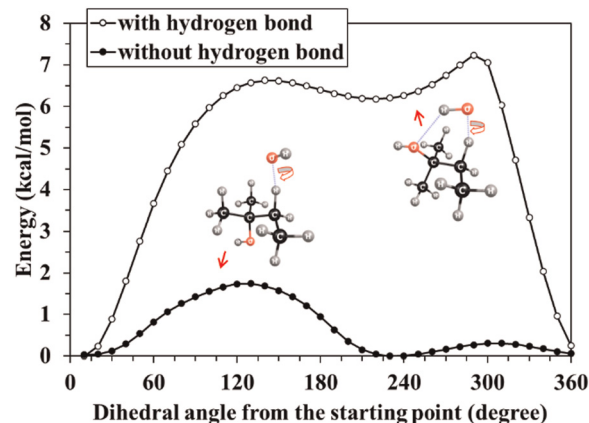


Fig. 3 Rotational potentials obtained at the M06-2X/6-31G level of theory for the same C–O torsional mode on the TS for the s- β H-atom abstraction reaction channel with and without hydrogen bonds, respectively.

the inner TS, and the van der Waals complex and products, respectively, were employed as well depths in the Eckart tunneling model. In general, the electronic energies of TSs for all H-atom abstraction reactions of 2M2B by $\bullet\text{OH}$ are quite close to those of the reactants and are even lower, indicating the necessity of the variational correction. The s- β H-atom abstraction reaction channel has the lowest energy barrier of -2.0 kcal mol^{-1} , while the H-atom abstraction reaction from the hydroxyl group has the highest energy barrier of 1.6 kcal mol^{-1} , and the energy barriers for the p- β and γ H-atom abstraction reactions lie in between. The TS conformers with hydrogen bonds stay lower in energy than those without hydrogen bonds by 1.5 – 3.0 kcal mol^{-1} , which is attributed to the stabilization effect of the formation of hydrogen bonds. In addition, the effect of hydrogen bonds on the torsional and vibrational modes of the TS is also observed. Being locked by the hydrogen bond, the rotational energy barriers of the C–C and C–O typically increase by 5 kcal mol^{-1} or larger, *e.g.*, Fig. 3, which decreases their contributions to the overall TS partition function. Moreover, the vibrational degrees of freedom of the TS will also be affected by the ring strain. For example, Table 2 shows the calculated normal mode vibrational frequencies of the two different types of TS conformers for the H-atom abstraction reaction from the s- β site. The vibrational frequencies below 1000 cm^{-1} become higher in the presence of hydrogen bonds. With harmonic oscillator approximation implemented for the normal modes, the vibrational partition functions for the TS will decrease when frequencies increase.

VTST calculations were carried out for all H-atom abstraction reactions by $\bullet\text{OH}$. The minimum rate coefficients were determined variationally based on a number of transition state structures along the reaction coordinate (defined by the distance between the O atom in the $\bullet\text{OH}$ radical and the H atom being abstracted) obtained from the IRC calculations at an energy-resolved level. The minimum energy paths (MEPs) employed for the H-atom abstraction reaction channels from the carbon sites are shown in Fig. 4. When the TS structures

Table 2 The 47 normal mode vibrational frequencies (with those corresponding to the six torsional modes removed) obtained at the M06-2X/6-311++G(d,p) level of theory for the saddle point of the s- β H-atom abstraction reaction channel with a hydrogen bond (ν) and without a hydrogen bond (ν')

ν (cm^{-1}) (TS of s- β , with a hydrogen bond)	ν' (cm^{-1}) (TS of s- β , without a hydrogen bond)
138.44, 195.69, 257.57, 320.72, 369.66, 410.94	83.77, 145.27, 257.73, 328.59, 372.53, 415.27
462.23, 531.36, 680.33, 747.76, 877.41, 910.92	450.33, 524.77, 657.80, 749.87, 774.63, 908.52
939.45, 969.25, 1003.16, 1014.73, 1032.38	940.16, 980.00, 1008.09, 1049.54, 1059.02
1094.77, 1150.76, 1164.99, 1192.80, 1239.03	1097.34, 1162.71, 1206.88, 1239.68, 1293.74
1284.51, 1325.90, 1395.97, 1400.43, 1412.12	1338.85, 1350.73, 1390.79, 1403.36, 1412.51
1418.66, 1483.74, 1485.20, 1496.63, 1499.37	1420.58, 1484.17, 1488.91, 1493.45, 1500.50
1505.06, 1519.59, 1556.88, 3052.74, 3056.79	1507.88, 1520.87, 1549.55, 3052.56, 3057.36
3059.26, 3097.61, 3123.36, 3127.87, 3130.20	3061.38, 3095.79, 3125.03, 3130.07, 3133.09
3149.47, 3152.26, 3154.05, 3751.05, 3889.20	3138.97, 3146.41, 3153.07, 3799.67, 3882.43

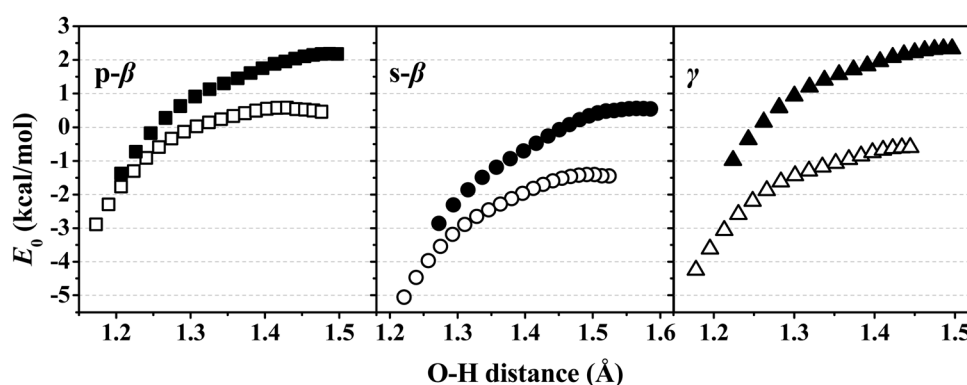


Fig. 4 ZPE corrected minimum energy paths obtained from IRC calculations at the M06-2X/6-311++G(d,p) level of theory for the H-atom abstraction reactions from the carbon sites of 2M2B. Solid symbols are electronic energies for the TS structures without hydrogen bonds, while open symbols are those for TS structures with hydrogen bonds.

without a hydrogen bond were used, the MEPs for the reactions are shifted upward by $\sim 2 \text{ kcal mol}^{-1}$ in energy, which will decrease the rate coefficients, especially at low temperatures. However, contributions from the internal C-C and C-O rotations and the normal mode vibrations (especially those below

1000 cm^{-1}) to the overall molecular partition functions of the TS also increase, which can significantly accelerate the rate constants at higher temperatures. The overall influence of the hydrogen bond formed in the TS on the calculated rate

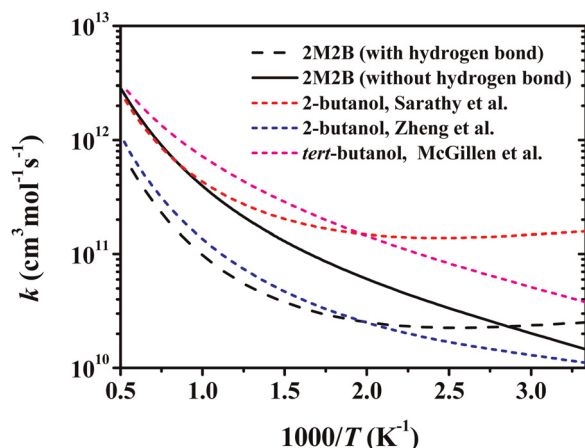


Fig. 5 Rate coefficients (per hydrogen atom) for the p- β H-atom abstraction reaction channel of 2M2B calculated in this study, 2-butanol from Sarathy *et al.*⁴⁹ and Zheng *et al.*,⁵⁰ and *tert*-butanol from McGillen *et al.*,⁵¹ respectively.

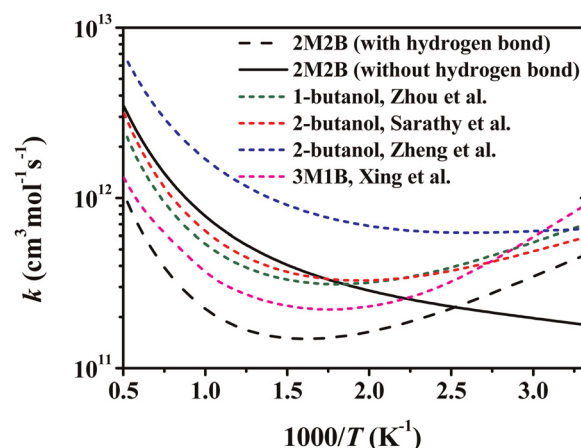


Fig. 6 Rate coefficients (per hydrogen atom) for the s- β H-atom abstraction reaction channel of 2M2B calculated in this study, 1-butanol from Zhou *et al.*,⁴⁸ 2-butanol from Zheng *et al.*⁵⁰ and Sarathy *et al.*,⁴⁹ and 3-methyl-1-butanol (3M1B) from Xing *et al.*,²⁰ respectively.

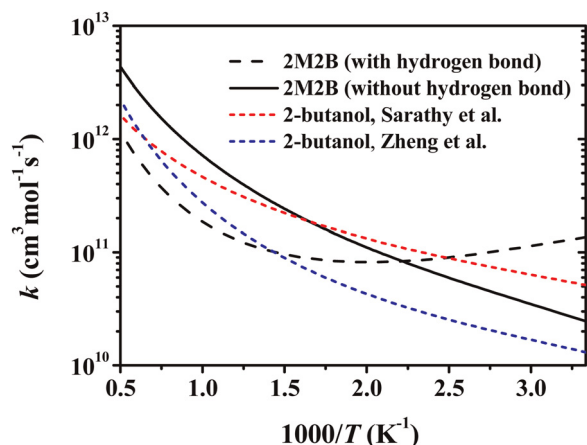


Fig. 7 Rate coefficients (per hydrogen atom) for the γ H-atom abstraction reaction channel of 2M2B calculated in this study, and 2-butanol from Sarathy *et al.*⁴⁹ and Zheng *et al.*⁵⁰ respectively.

coefficients is determined by their counter-balancing at different temperatures.

Fig. 5–7 show the calculated rate coefficients in this study for the p- β , s- β and γ H-atom abstraction reaction channels, respectively, in comparison with the reported rate coefficients in the literature for similar reaction pathways of other alcohol molecules. Note that the rate coefficients obtained in this study by using both TSs with a hydrogen bond and alternatively those without a hydrogen bond are shown. Since the TSs with a hydrogen bond all stay quite close to or below the reactants in energy, the corresponding rate coefficients exhibit a negative slope against temperature at temperatures below ~ 500 K. Moreover, the reaction kinetics is dominated by the energy barrier at lower temperatures, and the ratio of rate constants for the same reaction channel with/without a hydrogen bond in the TS can be 2–5 at 300 K, whereas at temperatures above 500 K, the effects of energy barrier start to be overtaken by the effects of partition functions, and the rate coefficients calculated by

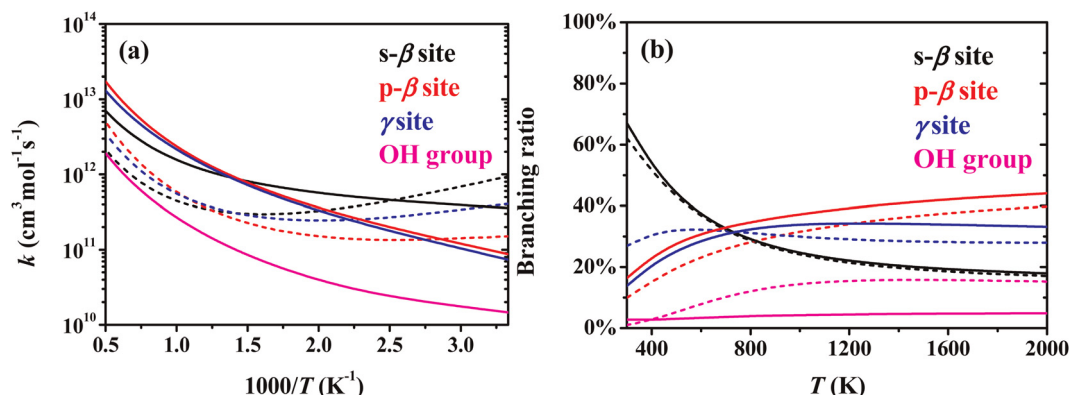


Fig. 8 (a) Rate coefficients for the H-atom abstraction reactions of 2M2B and the corresponding (b) branching ratios. Solid lines are the results obtained by employing TS structures without hydrogen bonds, while dashed lines are the results for TS structures with hydrogen bonds.

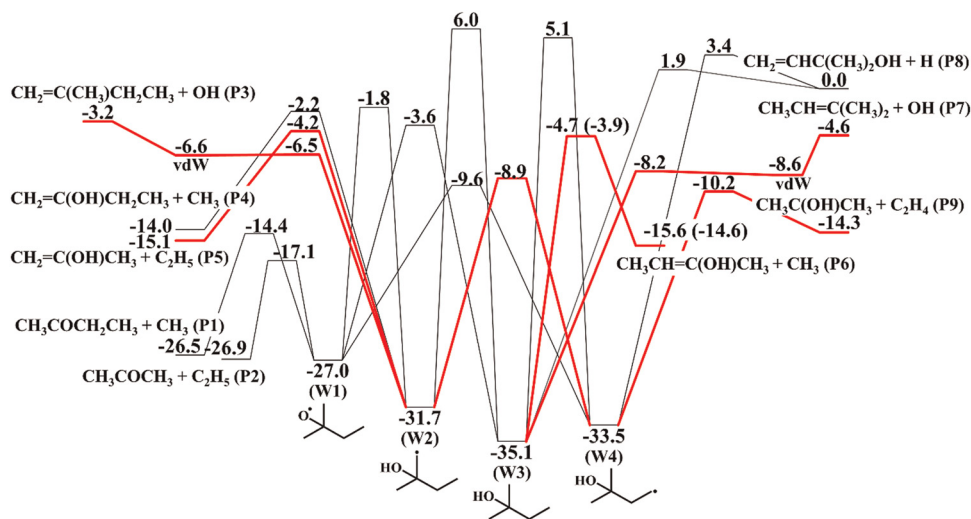


Fig. 9 ZPE corrected PESSs (in units of kcal mol^{-1}) for the unimolecular isomerization and β -scission reactions of 2M2B radicals at the QCISD(T)/CBS//M06-2X/6-311++G(d,p) level (with important reaction channels in red). The relative energies for W3 = P6 (*cis*) are in parentheses.

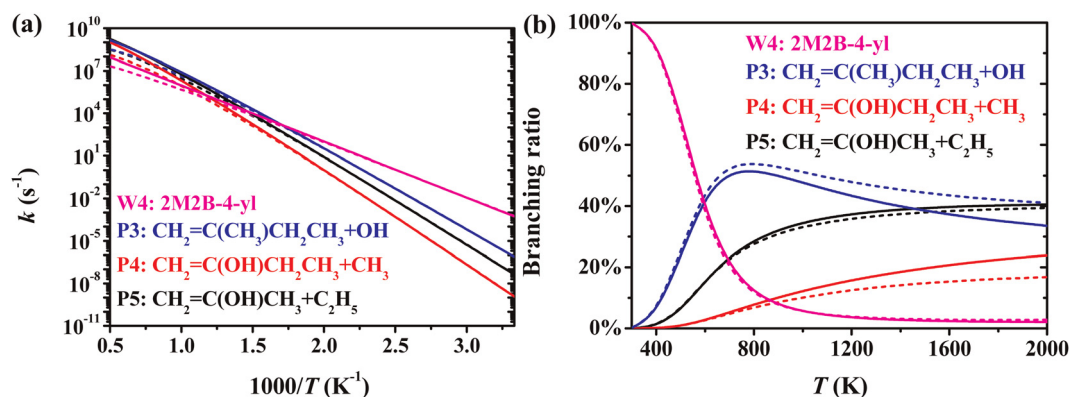


Fig. 10 Pressure-dependent (a) rate coefficients and (b) product branching ratios for the unimolecular reactions of 2M2B-1-yl (W2). Solid lines: 10 atm, dashed lines: 1 atm.

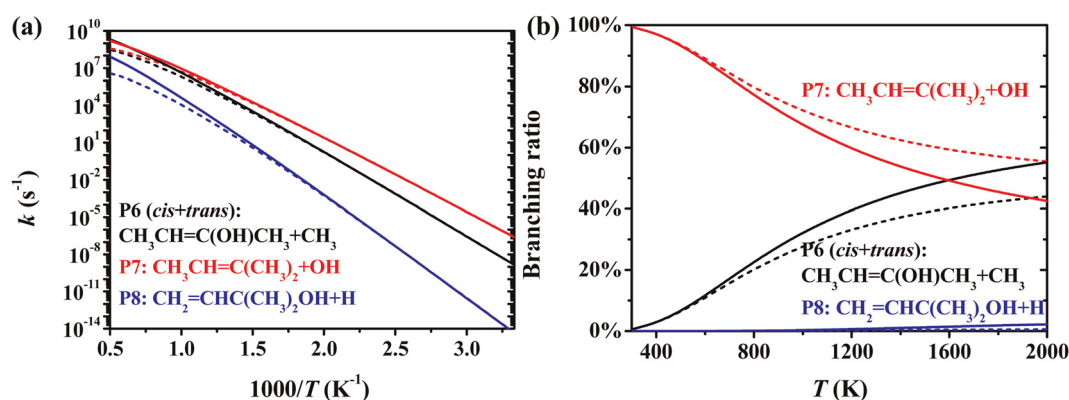


Fig. 11 Pressure-dependent (a) rate coefficients and (b) product branching ratios for the unimolecular reactions of 2M2B-3-yl (W3). Solid lines: 10 atm, dashed lines: 1 atm.

employing the TS without a hydrogen bond become ~ 2 times higher. In terms of site-specific reaction kinetics, our calculated rate coefficients for 2M2B based on the TS structures without hydrogen bonds are found to be more consistent with those for similar reaction pathways of 1-butanol,⁴⁸ 2-butanol,^{49,50} *tert*-butanol⁵¹ and 3-methyl-1-butanol (3M1B)²⁰ at temperatures above 500 K.

The calculated rate coefficients for all H-atom abstraction reactions of 2M2B by \bullet OH and their branching ratios are shown in Fig. 8. The s- β H-atom abstraction reaction channel forming 2M2B-3-yl is the most important at temperatures below 700 K because of its lowest energy barrier. While at temperatures of 1000 K or higher, the p- β and γ H-atom abstraction reaction pathways forming 2M2B-1-yl and 2M2B-4-yl, respectively, are more competitive, with the first pathway being slightly faster. Abstraction of the hydrogen atom from the hydroxyl group by \bullet OH is the slowest throughout 300–2000 K and the formation of 2-methyl-2-butoxy is marginal. When employing the TS structures without hydrogen bonds for the H-atom abstraction reaction pathways from the carbon sites, the relative importance of the p- β and γ H-atom abstraction reaction channels is

slightly enhanced at temperatures above 1000 K and the ratio to the hydroxyl group channel becomes negligible.

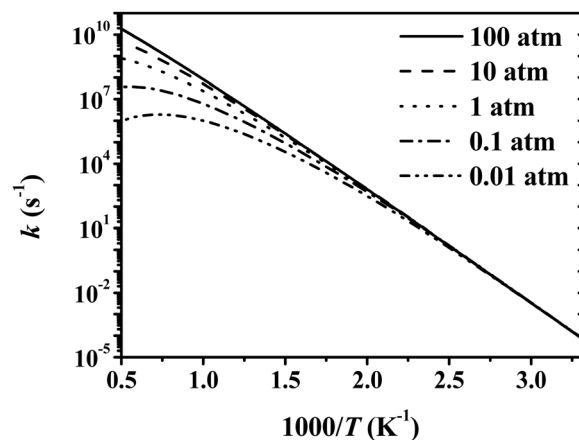


Fig. 12 Pressure-dependent rate coefficients for 2M2B-4-yl (W4) = CH₃C(OH)CH₃ + C₂H₄ (P9).

Table 3 The calculated standard formation enthalpy ($\Delta_f H_{298}^\ominus$) and entropy (S_{298}^\ominus) for each species in title reactions in comparison with literature data

Species	$\Delta_f H_{298}^\ominus$ [kcal mol ⁻¹]		S_{298}^\ominus [cal mol ⁻¹ K ⁻¹]	
	This study	Literature	This study	Literature
2-Butanone (P11)	-57.0	-57.0 ± 0.2 ^a , -57.0 ± 0.2 ^b , -56.9 ^b , -57.0 ^c	81.2	81.3 ^c
Methyl (P12)	35.1	35.0 ^a , 34.8 ^b , 35.1 ± 0.2 ^b , 35.1 ^c	46.7	46.4 ^b , 46.4 ^c
Acetone (P21)	-51.8	-51.8 ± 0.1 ^a , -51.9 ± 0.1 ^b , -52.0 ± 0.2 ^b , -51.7 ^b	70.6	
Ethyl (P22)	28.7	28.7 ± 0.1 ^a , 28.4 ± 0.5 ^b , 28.6 ± 0.1 ^c	60.6	60.5, ²¹ 58.1 ^c
2-Methyl-1-butene (P31)	-8.5	-8.4 ± 0.2 ^b , -8.3 ^b , -8.7 ^c	82.3	81.2 ^c
Hydroxyl (P32)	9.1	9.0 ^a , 9.3 ^b , 8.9 ± 0.1 ^c	43.8	43.9 ^b , 43.9 ^c
1-Buten-2-ol (P41)	-45.2		78.7	
Propen-2-ol (P51)	-40.6		69.4	
<i>trans</i> -2-Buten-2-ol (P61)	-46.7	-51.1 ^b	79.4	
<i>cis</i> -2-Buten-2-ol (P61)	-45.6	-50.7 ^b	79.0	
2-Methyl-2-butene (P71)	-10.1	9.9 ± 0.2 ^b , 9.8 ^b , -10.2 ^c	80.4	80.9 ^b
2-Methyl-3-buten-2-ol (P81)	-49.2		85.8	
2-Hydroxyl-2-propyl (P91)	-23.8		76.8	
Ethylene (P92)	12.5	12.5 ^a , 12.5 ^b , 12.5 ± 0.1 ^b , 12.5 ^c	52.3	52.4 ^b , 52.4 ^c
2-Methyl-2-butoxy (W1)	-25.9		88.2	
2M2B-1-yl (W2)	-29.9		93.2	
2M2B-3-yl (W3)	-33.2		91.6	
2M2B-4-yl (W4)	-31.7		92.4	
2M2B	-79.9	-78.7 ^b	89.9	86.7 ± 1.6 ^b

^a Active Thermochemical Tables (Branko Ruscic Argonne National Lab).⁵³ ^b NIST Chemistry Webbook.⁵⁴ ^c Third Millennium Ideal Gas and Condensed Phase Thermochemical Database for combustion (Burcat).⁵⁵

3.2. H₂O elimination reactions

2M2B molecules can undergo two different dehydration reaction pathways forming 2-methyl-1-butene and 2-methyl-2-butene, with energy barriers of 62.4 and 64.0 kcal mol⁻¹, respectively. The calculated energy barriers for the dehydration reactions of 2M2B are in good agreement with the average value, 62.4 kcal mol⁻¹, derived for this reaction class from a series of C₂-C₄ alcohols by Carstensen and Dean.⁵² Given that the number of p-β H atoms is three times the number of s-β H atoms, the formation of 2-methyl-1-butene + H₂O is faster than that of 2-methyl-2-butene + H₂O at various temperatures and pressures.

3.3. Isomerization and β-scission reactions of 2M2B radicals

The ZPE corrected PESs calculated at the QCISD(T)/CBS//M06-2X/6-311++G(d,p) level of theory for the unimolecular isomerization and β-scission reactions of the four 2M2B radicals, 2-methyl-2-butoxy (W1), 2M2B-1-yl (W2), 2M2B-3-yl (W3) and 2M2B-4-yl (W4), are shown in Fig. 9. For 2M2B-1-yl and 2M2B-3-yl, the C-O bond breaking will proceed through a TS with lower electronic energy compared to the products of alkene + •OH. Hence, a van der Waals product complex was located for each of them, and variational corrections were employed for their TSs. The β C-C bond decomposition reaction of 2M2B-3-yl can proceed through two distinct TSs and form *trans*- and *cis*-2-buten-2-ol + •CH₃ (P6), respectively. They were considered as separate reaction channels in our calculations, with the energy barrier for the *cis* TS being 0.8 kcal mol⁻¹ higher. For 2-methyl-2-butoxy, the β-scission reaction pathways are predominantly favoured because of their significantly lower energy barriers compared with those of isomerization pathways. The formation of 2-methyl-1-butene + •OH and 2-methyl-2-butene + •OH is energetically favoured for 2M2B-1-yl and

2M2B-3-yl, respectively. For 2M2B-4-yl, the β C-C bond breaking to form 2-hydroxyl-2-propyl + ethylene has the lowest energy barrier. Although the energy barriers for the isomerization channels through a five-membered ring TS, 2-methyl-2-butoxy ↔ 2M2B-4-yl and 2M2B-1-yl ↔ 2M2B-4-yl, are relatively low, these reaction channels are expected to be less important at high temperatures because of the entropy cost associated with the ring formed in the TS.

For 2-methyl-2-butoxy, the β-scission reactions dominated over the entire temperature range from 300 to 2000 K, consistent with their considerably lower energy barriers, with the formation processes of acetone + ethyl (P2) and 2-butanone + methyl (P1) competing with each other. The calculated rate coefficients for the unimolecular reactions of 2M2B-1-yl as well as the product branching ratios at 1 and 10 atm are shown in Fig. 10. At temperatures below 600 K, 2M2B-1-yl predominantly isomerizes to 2M2B-4-yl, because of the lower energy barrier of 22.8 kcal mol⁻¹, while at higher temperatures the β-scission reactions of 2M2B-1-yl producing 2-methyl-1-butene + •OH (P3) and propen-2-ol + •C₂H₅ (P5) become more competitive. When the pressure increases from 1 to 10 atm, the relative yield of 1-buten-2-ol + •CH₃ (P4) is slightly enhanced.

For the unimolecular reactions of 2M2B-3-yl, as illustrated in Fig. 11, the main products are *trans*- and *cis*-2-buten-2-ol + •CH₃ (P6) and 2-methyl-2-butene + •OH (P7), while the formation of 2-methyl-3-buten-2-ol + H• (P8) is negligible because of the pronouncedly higher energy barrier. The formation of 2-methyl-2-butene + •OH dominates at temperatures below 1200 K, while the formation of 2-buten-2-ol + •CH₃ shows some significance at 1500 K and above. At higher pressures the relative importance of production shifts slightly from 2-methyl-2-butene + •OH to 2-buten-2-ol + •CH₃ at high temperatures.

2M2B-4-yl almost completely decomposes to 2-hydroxyl-2-propyl + ethylene (P9) under combustion relevant temperatures

Table 4 Comparison of the calculated heat capacity (C_p) for each species in title reactions with literature data

Species	$C_p(T)$ [cal mol ⁻¹ K ⁻¹]						
2-Butanone (P11)	300	400	500	600	800	1000	1500
	24.4	29.2	33.7	37.9	44.8	50.1	58.5
	24.4 ^b	29.7 ^b	34.7 ^b	39.0 ^b	46.0 ^b	51.1 ^b	59.1 ^b
	24.5 ^c						
Methyl (P12)	9.6	10.2	10.9	11.6	12.8	13.9	16.1
	9.3 ^b	10.1 ^b	10.8 ^b	11.5 ^b	12.9 ^b	14.1 ^b	16.3 ^b
	9.2 ^c						
Acetone (P21)	17.4	21.3	25.1	28.6	34.0	38.1	44.5
	18.0 ^b	22.0 ^b	25.8 ^b	29.2 ^b	34.7 ^b	38.7 ^b	45.1 ^b
Ethyl (P22)	12.2	14.6	17.0	19.2	22.6	25.4	29.9
	12.1 ^c						
2-Methyl-1-butene (P31)	25.7	32.1	38.2	43.6	51.8	58.2	68.1
	26.4 ^b	33.2 ^b	39.4 ^b	44.7 ^b	53.2 ^b	59.4 ^b	69.1 ^b
	26.2 ^c						
Hydroxyl (P32)	7.2	7.1	7.0	7.0	7.1	7.2	7.7
	7.2 ^b	7.1 ^b	7.1 ^b	7.1 ^b	7.2 ^b	7.3 ^b	7.9 ^b
	7.1 ^c						
1-Buten-2-ol (P41)	25.1	31.5	37.0	41.4	47.5	52.0	59.3
Propen-2-ol (P51)	20.0	24.7	28.8	32.0	36.4	39.7	45.1
<i>trans</i> -2-Buten-2-ol (P61)	25.0	30.2	34.9	39.1	45.6	50.6	58.5
<i>cis</i> -2-Buten-2-ol (P61)	24.6	30.3	35.3	39.6	45.9	50.8	58.7
2-Methyl-2-butene (P71)	24.8	30.9	36.9	42.3	50.8	57.4	67.6
	25.2 ^b	31.9 ^b	38.1 ^b	43.4 ^b	52.1 ^b	58.5 ^b	68.6 ^b
	25.1 ^c						
2-Methyl-3-buten-2-ol (P81)	31.9	39.0	45.2	50.3	58.0	63.8	73.1
2-Hydroxyl-2-propyl (P91)	21.1	25.0	28.9	32.3	37.7	41.9	48.5
Ethylene (P92)	10.1	12.3	14.5	16.6	19.6	22.1	25.9
	10.3 ^b	12.7 ^b	14.9 ^b	16.9 ^b	20.0 ^b	22.4 ^b	26.3 ^b
	10.3 ^c						
2-Methyl-2-butoxy (W1)	31.8	39.4	46.1	52.0	60.8	67.5	78.0
2M2B-1-yl (W2)	34.0	41.2	47.5	52.9	61.1	67.3	77.3
2M2B-3-yl (W3)	35.4	42.1	47.8	52.7	60.7	66.9	77.0
2M2B-4-yl (W4)	33.3	40.5	47.1	52.7	61.0	67.3	77.3
2-Methyl-2-butanol	33.0	40.8	47.9	54.1	63.4	70.5	81.7
		41.1 ^b	47.8 ^b				

^a Active Thermochemical Tables (Branko Ruscic Argonne National Lab).⁵³ ^b NIST Chemistry Webbook.⁵⁴ ^c Third Millennium Ideal Gas and Condensed Phase Thermochemical Database for Combustion (Burcat).⁵⁵

and pressures. The calculated pressure-dependent rate coefficients for the formation of 2-hydroxyl-2-propyl + ethylene are shown in Fig. 12. Similar to the rate coefficients for the other β -scission reactions investigated here, the pressure fall-off effect of the kinetics of this reaction channel is more pronounced at pressures below 1 atm and temperatures above 500 K.

3.4. Thermochemistry

The calculated enthalpies of formation ($\Delta_f H_{298}^\ominus$) and entropies (S_{298}^\ominus) under standard conditions are shown in Table 3, compared with the available data from the Active Thermochemical Tables (ATcT),⁵³ the NIST Chemistry Webbook⁵⁴ and the Third Millennium Ideal Gas and Condensed Phase Thermochemistry Database for Combustion (Burcat database).⁵⁵ Heat capacities (C_p) at various temperatures are shown in Table 4. The calculated standard formation enthalpies are in excellent agreement with the available benchmark values in ATcT, all within 0.2 kcal mol⁻¹. In general, the deviations of our standard formation enthalpy results from the available data in NIST and Burcat databases are no larger than 1.2 kcal mol⁻¹, except for the

standard formation enthalpy of *trans*-2-buten-2-ol and *cis*-2-buten-2-ol. The formation enthalpy for *trans*- and *cis*-2-buten-2-ol in the NIST database was measured by Turecek *et al.*,⁵⁶ being ~ 5 kcal mol⁻¹ lower than our calculated one. Moreover, the estimated value by using Benson's group additivity method reported in ref. 56 was -49.5 kcal mol⁻¹, which is also lower by 2.8 kcal mol⁻¹. On the other hand, the calculated entropies at 298 K are in reasonable agreement with the literature data. The calculated heat capacities also agree well with the available data in the literature, with a maximum deviation of 1.4 cal mol⁻¹ K⁻¹ over temperatures from 300 to 1500 K.

4. Conclusions

The kinetics of the important oxidation reactions of 2-methyl-2-butanol (2M2B) were studied in this study by performing high-level *ab initio* calculations. Rate coefficients for H-atom abstraction reactions from the primary β (p- β), secondary β (s- β) and γ sites of 2M2B were obtained by employing the transition state structures with and without hydrogen bonds separately, to analyse the effect of hydrogen bond formation in the TS on the reaction kinetics. The rate coefficients calculated by using the TS structures with hydrogen bonds are higher at temperatures below ~ 400 K because of the lower energy barrier, whereas under combustion relevant temperature regimes, the rate coefficients obtained from the TSs without hydrogen bonds are higher. The s- β H-atom abstraction reaction channel is dominant at temperatures below 700 K, while the p- β and γ H-atom abstraction reaction channels are more competitive at 1000 K and above. For all the unimolecular reactions studied, pressure-dependent rate coefficients were obtained from the solution of RRKM/ME, and the important product channels for each 2M2B radical were identified through their branching ratios. Temperature-dependent thermochemical data for all the species involved in the title reactions were calculated, which are found to be in good agreement with the available data in the literature.

Conflicts of interest

■■■■■

Acknowledgements

The work at Beihang University was supported by the National Science and Technology Major Project (2017-III-0004-0028) and Sinopec Science and Technology Department. The computational resources for this work were provided by the High-performance computing centre (HPC) at Beihang University.

References

- 1 K. Kohse-Höinghaus, P. Oßwald, T. A. Cool, T. Kasper, N. Hansen, F. Qi, C. K. Westbrook and

- 1 P. R. Westmoreland, *Angew. Chem., Int. Ed.*, 2010, **49**, 3572–3597.
- 2 S. M. Sarathy, P. Oßwald, N. Hansen and K. Kohse-Höinghaus, *Prog. Energy Combust. Sci.*, 2014, **44**, 40–102.
- 5 3 Y. Yang, J. Dec, N. Dronniou and B. Simmons, *SAE Int. J. Fuels Lubr.*, 2010, **3**, 725–741.
- 4 M. Lapuerta, R. García-Contreras, J. Campos-Fernández and M. P. Dorado, *Energy Fuels*, 2010, **24**, 4497–4502.
- 5 B. Rajesh Kumar and S. Saravanan, *Fuel*, 2016, **170**, 49–59.
- 10 6 Z.-H. Zhang and R. Balasubramanian, *Appl. Energy*, 2016, **163**, 71–80.
- 7 A. F. Cann and J. C. Liao, *Appl. Microbiol. Biotechnol.*, 2010, **85**, 893–899.
- 15 8 L. Cai, F. vom Lehn and H. Pitsch, *Energy Fuels*, 2021, **35**, 1890–1917.
- 9 K. A. Heufer, S. M. Sarathy, H. J. Curran, A. C. Davis, C. K. Westbrook and W. J. Pitz, *Energy Fuels*, 2012, **26**, 6678–6685.
- 20 10 C. Togbé, F. Halter, F. Foucher, C. Mounaim-Rousselle and P. Dagaut, *Proc. Combust. Inst.*, 2011, **33**, 367–374.
- 11 Z. Serinyel, C. Togbé, G. Dayma and P. Dagaut, *Combust. Flame*, 2014, **161**, 3003–3013.
- 12 G. Dayma, C. Togbé and P. Dagaut, *Energy Fuels*, 2011, **25**, 4986–4998.
- 25 13 M. Köhler, T. Kathrotia, P. Oßwald, M. L. Fischer-Tammer, K. Moshhammer and U. Riedel, *Combust. Flame*, 2015, **162**, 3197–3209.
- 14 C. Cao, Y. Zhang, X. Zhang, J. Zou, F. Qi, Y. Li and J. Yang, *Fuel*, 2019, **257**, 116039.
- 30 15 Q. Li, C. Tang, Y. Cheng, L. Guan and Z. Huang, *Energy Fuels*, 2015, **29**, 5334–5348.
- 16 R. Jalain, J. Bonnetty, G. Legros and A. Matynia, *Fuel*, 2022, **307**, 121793.
- 35 17 L. Zhao, L. Ye, F. Zhang and L. Zhang, *J. Phys. Chem. A*, 2012, **116**, 9238–9244.
- 18 B. Azaad and S. Lakshmipathi, *Mol. Phys.*, 2018, **116**, 1153–1165.
- 19 R. Van de Vijver, K. M. Van Geem, G. B. Marin and J. Zádor, *Combust. Flame*, 2018, **196**, 500–514.
- 40 20 L. Xing, Z. Wang and D. G. Truhlar, *J. Am. Chem. Soc.*, 2019, **141**, 18531–18543.
- 21 J. Bai, Y. Zhu, C.-W. Zhou, G. Dayma, Z. Serinyel and P. Dagaut, *Proc. Combust. Inst.*, 2021, **38**, 823–832.
- 45 22 F.-Y. Bai, M.-Y. Chen, X.-H. Liu, S. Ni, Y.-Z. Tang, X.-M. Pan and Z. Zhao, *New J. Chem.*, 2021, **45**, 16543–16556.
- 23 Y. Zhao and D. G. Truhlar, *Theor. Chem. Acc.*, 2008, **120**, 215–241.
- 24 A. D. McLean and G. S. Chandler, *J. Chem. Phys.*, 1980, **72**, 5639.
- 50 25 C. Hampel, K. A. Peterson and H.-J. Werner, *Chem. Phys. Lett.*, 1992, **190**, 1–12.
- 26 T. H. Dunning, *J. Chem. Phys.*, 1989, **90**, 1007–1023.
- 27 R. A. Kendall, T. H. Dunning Jr and R. J. Harrison, *J. Chem. Phys.*, 1992, **96**, 6796–6806.
- 28 M. Head-Gordon, J. A. Pople and M. J. Frisch, *Chem. Phys. Lett.*, 1988, **153**, 503–506.
- 29 D. E. Woon and T. H. Dunning Jr, *J. Chem. Phys.*, 1993, **98**, 1358–1371.
- 30 P. Zhang, S. J. Klippenstein and C. K. Law, *J. Phys. Chem. A*, 2013, **117**, 1890–1906.
- 31 H.-J. Werner, P. J. Knowles and G. Knizia, *et al.*, *MOLPRO, version 2015.1, a package of ab initio programs*, see <http://www.molpro.net>.
- 32 <https://github.com/Auto-Mech> [accessed 21.09.23].
- 10 33 Y. Georgievskii, J. A. Miller, M. P. Burke and S. J. Klippenstein, *J. Phys. Chem. A*, 2013, **117**, 12146–12154.
- 34 C. Eckart, *Phys. Rev.*, 1930, **35**, 1303.
- 35 F. M. Mourits and F. H. A. Rummens, *Can. J. Chem.*, 1977, **55**, 3007–3020.
- 15 36 S. J. Klippenstein and J. A. Miller, *J. Phys. Chem. A*, 2005, **109**, 4285–4295.
- 37 M. Keçeli, S. N. Elliott, Y.-P. Li, M. S. Johnson, C. Cavallotti, Y. Georgievskii, W. H. Green, M. Pelucchi, J. M. Wozniak, A. W. Jasper and S. J. Klippenstein, *Proc. Combust. Inst.*, 2019, **37**, 363–371.
- 20 38 J. W. Ochterski, G. A. Petersson and J. A. Montgomery, *J. Chem. Phys.*, 1996, **104**, 2598–2619.
- 39 J. A. Montgomery, M. J. Frisch, J. W. Ochterski and G. A. Petersson, *J. Chem. Phys.*, 2000, **112**, 6532–6542.
- 25 40 L. A. Curtiss, K. Raghavachari, P. C. Redfern, V. Rassolov and J. A. Pople, *J. Chem. Phys.*, 1998, **109**, 7764–7776.
- 41 L. A. Curtiss, P. C. Redfern and K. Raghavachari, *J. Chem. Phys.*, 2007, **126**, 084–108.
- 30 42 J. M. Simmie and K. P. Somers, *J. Phys. Chem. A*, 2015, **119**, 7235–7246.
- 43 B. J. McBride and S. D. Gordon, *Computer program for calculating and fitting thermodynamic functions*, 1992.
- 44 B. Rotavera and C. A. Taatjes, *Prog. Energy Combust. Sci.*, 2021, **86**, 100925.
- 35 45 C. W. Zhou, J. M. Simmie and H. J. Curran, *Int. J. Chem. Kinet.*, 2012, **44**, 155–164.
- 46 Y. Georgievskii and S. J. Klippenstein, *J. Phys. Chem. A*, 2007, **111**, 3802–3811.
- 40 47 S. Xu, R. Zhu and M.-C. Lin, *Int. J. Chem. Kinet.*, 2006, **38**, 322–326.
- 48 C.-W. Zhou, J. M. Simmie and H. J. Curran, *Combust. Flame*, 2011, **158**, 726–731.
- 49 S. M. Sarathy, S. Vranckx, K. Yasunaga, M. Mehl, P. Oßwald, W. K. Metcalfe, C. K. Westbrook, W. J. Pitz, K. Kohse-Höinghaus and R. X. Fernandes, *Combust. Flame*, 2012, **159**, 2028–2055.
- 50 J. Zheng, G. A. Oyedepo and D. G. Truhlar, *J. Phys. Chem. A*, 2015, **119**, 12182–12192.
- 50 51 M. R. McGillen, M. Baasandorj and J. B. Burkholder, *J. Phys. Chem. A*, 2013, **117**, 4636–4656.
- 52 H.-H. Carstensen and A. M. Dean, *Computational modeling in lignocellulosic biofuel production*, ACS Publications, 2010, pp.201–243.
- 55

1	53	B. Ruscic and D. H. Bross, Active Thermochemical Tables (ATcT) values based on ver. 1.122r of the Thermochemical Network, 2021.	55	A. Burcat and B. Ruscic, Chemistry and T. I. I. of Tech, Third millenium ideal gas and condensed phase thermochemical database for combustion (with update from active thermochemical tables), 2005.	1
5	54	C. E. Lemmon, M. McLinden, D. Friend and W. M. P. Linstrom, <i>NIST Chemistry Webbook, NIST Standard Reference Database Number 69</i> , National Institute of Standards and Technology, Gaithersburg, 2021.	56	F. Turecek, L. Brabec and J. Korvola, <i>J. Am. Chem. Soc.</i> , 1988, 110 , 7984–7990.	5
10					10
15					15
20					20
25					25
30					30
35					35
40					40
45					45
50					50
55					55

Dear Author

Please use this PDF proof to check the layout of your article. If you would like any changes to be made to the layout, you can leave instructions in the online proofing interface. First, return to the online proofing interface by clicking "Edit" at the top of the page, then insert a Comment in the relevant location. Making your changes directly in the online proofing interface is the quickest, easiest way to correct and submit your proof.

Please note that changes made to the article in the online proofing interface will be added to the article before publication, but are not reflected in this PDF proof.